

Isospin effects in the disappearance of flow as a function of colliding geometry

Sakshi Gautam^a, Aman D. Sood^{b1}, Rajeev K. Puri^a, and J. Aichelin^b

^a*Department of Physics, Panjab University, Chandigarh -160 014, India.*

^b*SUBATECH, Laboratoire de Physique Subatomique et des Technologies Associées, Université de Nantes - IN2P3/CNRS - EMN 4 rue Alfred Kastler, F-44072 Nantes, France.*

We study the effect of isospin degree of freedom on the balance energy (E_{bal}) as well as its mass dependence throughout the mass range 48-270 for two sets of isobaric systems with $N/Z = 1$ and 1.4 at different colliding geometries ranging from central to peripheral ones. Our findings reveal the dominance of Coulomb repulsion in isospin effects on E_{bal} as well as its mass dependence throughout the range of the colliding geometry. Our results also indicate that the effect of symmetry energy and nucleon-nucleon cross section on E_{bal} is uniform throughout the mass range and throughout the colliding geometry. We also present the counter balancing of nucleon-nucleon collisions and mean field by reducing the Coulomb and the counter balancing of Coulomb and mean field by removing the nucleon-nucleon collisions.

¹Email: amandsood@gmail.com

1 Introduction

With the availability of radioactive ion beam (RIB) facilities at Cooler Storage Ring (CSR) (China) [1], the GSI Facility for Antiproton and Ion beam Research (FAIR) [2], RIB facility at Rikagaku Kenyusho (RIKEN) in Japan [3], GANIL in France [4], and the upcoming facility for RIB at Michigan State University [5] one has a possibility to study the properties of nuclear matter under the extreme conditions of isospin asymmetry. Heavy-ion collisions induced by the neutron rich matter provide a unique opportunity to explore the isospin dependence of in-medium nuclear interactions, since isospin degree of freedom plays an important role in heavy-ion collisions through both the nuclear matter equation of state (EOS) as well as via in-medium nucleon-nucleon (nn) cross section.

After about three decades of intensive efforts in both nuclear experiments and theoretical calculations, equation of state for isospin symmetric matter is now relatively well understood [6]. The effect of isospin degree of freedom on the collective transverse in-plane flow as well as on its disappearance [7] (there exists a particular incident energy called *balance energy* (E_{bal}) or *energy of vanishing flow* (EVF) at which transverse in-plane flow disappears) has been reported in the literature [8–10], where it was found that neutron-rich systems have higher E_{bal} compared to neutron-deficient systems at all colliding geometries varying from central to peripheral ones. The effect of isospin degree of freedom on E_{bal} was found to be much more pronounced at peripheral colliding geometries compared to central ones. As reported in the literature, the isospin dependence of collective flow as well as its disappearance has been explained as a competition among various reaction mechanisms, such as nucleon-nucleon collisions, symmetry energy, surface property of the colliding nuclei, and Coulomb force. The relative importance among these mechanisms is not yet clear [8]. In recent study, we [11] confronted theoretical calculations (using isospin-dependent quantum molecular dynamics (IQMD) model [12]) with the data at all colliding geometries and were able to reproduce the data within 5% on average at all colliding geometries. Motivated by the good agreement of the calculations with data, two of us [13] (in order to explore the relative importance among above mentioned reaction mechanisms in isospin effects on the E_{bal}) calculated the E_{bal} throughout the mass range for two sets of isotopic systems with $N/Z = 1.16$ and 1.33 . The isotopic pairs were chosen so that the effect of the Coulomb repulsion is the same for a given pair. The choice of the above N/Z was taken because the percentage difference $\Delta N/Z(\%) = \frac{(N/Z)^{1.33} - (N/Z)^{1.16}}{(N/Z)^{1.16}} \times 100$ between the

given pair is about 15% which is same as in Ref. [9, 11]. Based on the results of E_{bal} for isotopic pairs we concluded in Ref. [13] that mass dependence effects seem to dominate the isospin effects (consisting of isospin-dependent cross section, symmetry energy, surface properties). In our recent results [14] we find that collective flow for isotopic pairs with large difference between N/Z is sensitive to the symmetry energy. Coulomb repulsion will be same for isotopic pair throughout the mass range. The comparison of E_{bal} for isotopic pairs gave us the hint that the Coulomb repulsion could be dominant in isospin effects in collective flow as well as its disappearance [8, 9, 11]. Therefore Gautam and Sood [13] studied the isospin effects on the E_{bal} throughout the mass range 48-350 for two sets of isobaric systems with $N/Z = 1.0$ and 1.4 at semi central colliding geometry. These results showed that the difference between the E_{bal} for two isobaric systems is mainly due to the Coulomb repulsion. It was also shown that Coulomb repulsion dominates over symmetry energy. These findings also indicated towards the dominance of the Coulomb repulsion in larger magnitude of isospin effects in E_{bal} at peripheral collisions. Here we aim to extend the study over full range of colliding geometry varying from central to peripheral ones. Section 2 describes the model in brief. Section 3 explains the results and discussion and Sec. 4 summarizes the results.

2 The model

The present study is carried out within the framework of IQMD model [12]. The IQMD model treats different charge states of nucleons, deltas, and pions explicitly, as inherited from the Vlasov-Uehling-Uhlenbeck (VUU) model. The IQMD model has been used successfully for the analysis of a large number of observables from low to relativistic energies. The isospin degree of freedom enters into the calculations via symmetry potential, cross sections, and Coulomb interaction.

In this model, baryons are represented by Gaussian-shaped density distributions

$$f_i(\vec{r}, \vec{p}, t) = \frac{1}{\pi^2 \hbar^2} \exp(-[\vec{r} - \vec{r}_i(t)]^2 \frac{1}{2L}) \times \exp(-[\vec{p} - \vec{p}_i(t)]^2 \frac{2L}{\hbar^2}) \quad (1)$$

Nucleons are initialized in a sphere with radius $R = 1.12 A^{1/3}$ fm, in accordance with liquid-drop model. Each nucleon occupies a volume of h^3 , so that phase space is uniformly filled. The initial momenta are randomly chosen between 0 and Fermi momentum (\vec{p}_F). The nucleons of the target and projectile interact by two- and three-body Skyrme

forces, Yukawa potential, Coulomb interactions, and momentum-dependent interactions. In addition to the use of explicit charge states of all baryons and mesons, a symmetry potential between protons and neutrons corresponding to the Bethe-Weizsacker mass formula has been included. The hadrons propagate using Hamilton equations of motion:

$$\frac{d\vec{r}_i}{dt} = \frac{d\langle H \rangle}{d\vec{p}_i}; \quad \frac{d\vec{p}_i}{dt} = -\frac{d\langle H \rangle}{d\vec{r}_i} \quad (2)$$

with

$$\begin{aligned} \langle H \rangle &= \langle T \rangle + \langle V \rangle \\ &= \sum_i \frac{p_i^2}{2m_i} + \sum_i \sum_{j>i} \int f_i(\vec{r}, \vec{p}, t) V^{ij}(\vec{r}', \vec{r}) \\ &\quad \times f_j(\vec{r}', \vec{p}', t) d\vec{r} d\vec{r}' d\vec{p} d\vec{p}'. \end{aligned} \quad (3)$$

The baryon potential V^{ij} , in the above relation, reads as

$$\begin{aligned} V^{ij}(\vec{r}' - \vec{r}) &= V_{Skyrme}^{ij} + V_{Yukawa}^{ij} + V_{Coul}^{ij} + V_{mdi}^{ij} + V_{sym}^{ij} \\ &= [t_1 \delta(\vec{r}' - \vec{r}) + t_2 \delta(\vec{r}' - \vec{r}) \rho^{\gamma-1} (\frac{\vec{r}' + \vec{r}}{2})] \\ &\quad + t_3 \frac{\exp(|(\vec{r}' - \vec{r})|/\mu)}{(|(\vec{r}' - \vec{r})|/\mu)} + \frac{Z_i Z_j e^2}{|(\vec{r}' - \vec{r})|} \\ &\quad + t_4 \ln^2 [t_5 (\vec{p}' - \vec{p})^2 + 1] \delta(\vec{r}' - \vec{r}) \\ &\quad + t_6 \frac{1}{\rho_0} T_{3i} T_{3j} \delta(\vec{r}' - \vec{r}). \end{aligned} \quad (4)$$

Here Z_i and Z_j denote the charges of i th and j th baryon, and T_{3i} and T_{3j} are their respective T_3 components (i.e., $1/2$ for protons and $-1/2$ for neutrons). The parameters μ and t_1, \dots, t_6 are adjusted to the real part of the nucleonic optical potential. For the density dependence of the nucleon optical potential, standard Skyrme type parametrization is employed. The momentum-dependence V_{mdi}^{ij} of the nn interactions, which may optionally be used in IQMD, is fitted to the experimental data in the real part of the nucleon optical potential. It is worth mentioning that the Gaussian width which describes the interaction range of the particle depends on the mass of the system in IQMD, since each nucleus shows maximum stability for a particular width as shown in Ref. [11, 12]. For eg, width of Ca is 4.16 fm^2 and for Au is 8.33 fm^2 and Gaussian width varies between this mass range.

3 Results and discussion

For the present study, we simulate several thousands events of each reaction at incident energies around E_{bal} in small steps of 10 MeV/nucleon. In particular, we simulate the reactions $^{24}\text{Mg}+^{24}\text{Mg}$, $^{58}\text{Cu}+^{58}\text{Cu}$, $^{72}\text{Kr}+^{72}\text{Kr}$, $^{96}\text{Cd}+^{96}\text{Cd}$, $^{120}\text{Nd}+^{120}\text{Nd}$, $^{135}\text{Ho}+^{135}\text{Ho}$, having $N/Z = 1.0$ and reactions $^{24}\text{Ne}+^{24}\text{Ne}$, $^{58}\text{Cr}+^{58}\text{Cr}$, $^{72}\text{Zn}+^{72}\text{Zn}$, $^{96}\text{Zr}+^{96}\text{Zr}$, $^{120}\text{Sn}+^{120}\text{Sn}$, and $^{135}\text{Ba}+^{135}\text{Ba}$, having $N/Z = 1.4$, respectively, in the whole range of colliding geometry. The colliding geometry is divided into four impact parameter bins of $0.15 < \hat{b} < 0.25$ (BIN 1), $0.35 < \hat{b} < 0.45$ (BIN 2), $0.55 < \hat{b} < 0.65$ (BIN 3), and $0.75 < \hat{b} < 0.85$ (BIN 4), where $\hat{b} = b/b_{max}$. Here N/Z is changed by keeping the mass fixed. We use anisotropic standard isospin- and energy-dependent nn cross section $\sigma = 0.8 \sigma_{NN}^{free}$. The details about the elastic and inelastic cross sections for proton-proton and proton-neutron collisions can be found in Ref. [12]. The cross sections for neutron-neutron collisions are assumed to be equal to the proton-proton cross sections.

We also use soft equation of state along with momentum-dependent interactions (MDI). The results with the above choice of equation of state and cross section were in good agreement with the data [11, 13]. The reactions are followed until the transverse flow saturates. The saturation time varies from 100 fm/c for lighter masses to 300 fm/c for heavier masses. For transverse flow, we use the quantity "directed transverse momentum $\langle p_x^{dir} \rangle$ " which is defined as [15, 16]

$$\langle p_x^{dir} \rangle = \frac{1}{A} \sum_{i=1}^A \text{sign}\{y(i)\} p_x(i), \quad (5)$$

where $y(i)$ is the rapidity and $p_x(i)$ is the momentum of i^{th} particle. The rapidity is defined as

$$Y(i) = \frac{1}{2} \ln \frac{\mathbf{E}(i) + \mathbf{p}_z(i)}{\mathbf{E}(i) - \mathbf{p}_z(i)}, \quad (6)$$

where $\mathbf{E}(i)$ and $\mathbf{p}_z(i)$ are, respectively, the energy and longitudinal momentum of i^{th} particle. In this definition, all the rapidity bins are taken into account. A straight line interpolation is used to calculate E_{bal} .

Figure 1 displays the mass dependence of E_{bal} for four impact parameter bins. The solid (open) green circles indicate E_{bal} for systems with lower (higher) N/Z . Lines are power law fit $\propto A^\tau$. Left (right) panels are for mass dependence of E_{bal} when we include (exclude) $A = 48$. First we discuss the left panels for all the four bins. E_{bal} follows a

Table 1: The values of τ_1 and $\tau_{1.4}$ for BIN 1 to BIN 4 for calculations with Coulomb potential with and without A=48.

b/b _{max}	τ_1		$\tau_{1.4}$	
	With A=48	Without A=48	With A=48	Without A=48
BIN 1	-0.36± 0.01	-0.38± 0.03	-0.33± 0.01	-0.31± 0.02
BIN 2	-0.50± 0.01	-0.54± 0.03	-0.45± 0.01	-0.48± 0.01
BIN 3	-0.70± 0.03	-0.83± 0.07	-0.56± 0.02	-0.57± 0.07
BIN 4	-0.93± 0.08	-1.14± 0.25	-0.70± 0.01	-0.70± 0.03

Table 2: Same as table 1 but for calculations with Coulomb potential reduced by a factor of 100.

b/b _{max}	τ_1		$\tau_{1.4}$	
	With A=48	Without A=48	With A=48	Without A=48
BIN 1	-0.25± 0.02	-0.17± 0.02	-0.26± 0.03	-0.14± 0.01
BIN 2	-0.25± 0.02	-0.17± 0.02	-0.28± 0.02	-0.19± 0.02
BIN 3	-0.33± 0.02	-0.24± 0.03	-0.33± 0.02	-0.26± 0.01
BIN 4	-0.41± 0.02	-0.31± 0.03	-0.41± 0.02	-0.29± 0.02

power law behavior $\propto A^\tau$ for both $N/Z = 1$ and 1.4 (τ being labeled as $\tau_{1.0}$ and $\tau_{1.4}$ for systems having $N/Z = 1$ and 1.4 , respectively) at all colliding geometries. There are small deviations from power law behavior for heavy mass systems with $N/Z = 1$ at peripheral colliding geometry. Isospin effects are clearly visible for all the four bins as neutron-rich system has higher E_{bal} throughout the mass range in agreement with the previous studies [8, 9, 11].

The magnitude of isospin effects increases with increase in mass of the system at all colliding geometries. The effect is much more pronounced at larger colliding geometries. One can see that the difference between $\tau_{1.0}$ and $\tau_{1.4}$ increases with increase in the impact parameter (green circles). In Ref. [13], Gautam and Sood studied the isospin effects on the mass dependence of E_{bal} for BIN 2. There they reduced the Coulomb potential by a factor of 100 and showed that the Coulomb repulsion plays dominant role over symmetry

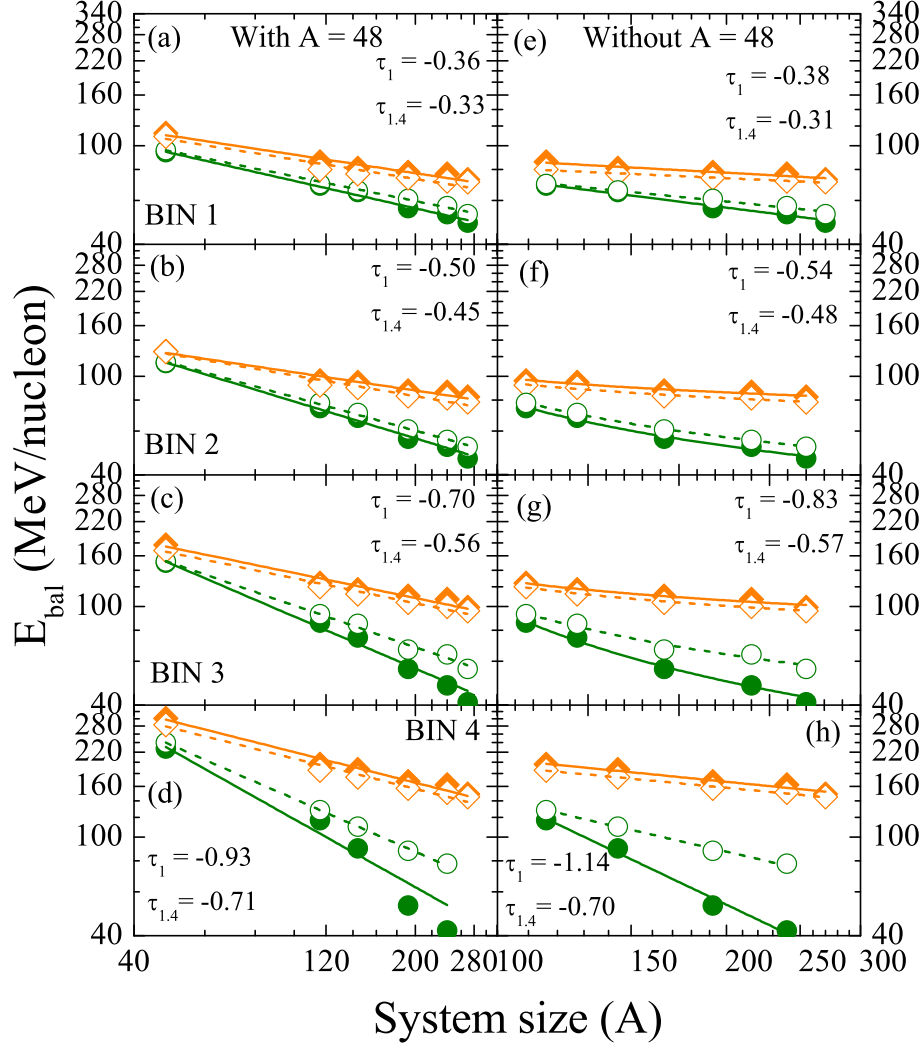


Figure 1: (Color online) Left (right) panels displays E_{bal} as a function of combined mass of system for different impact parameter bins with (without) $A = 48$. Solid (open) symbols are for systems having $N/Z = 1.0$ (1.4). Circles (diamonds) are for calculations with full (reduced) Coulomb. Lines are power law fit $\propto A^\tau$. τ values without errors for full Coulomb calculations are displayed in figure. The detailed values of τ are given in the table 1 and 2.

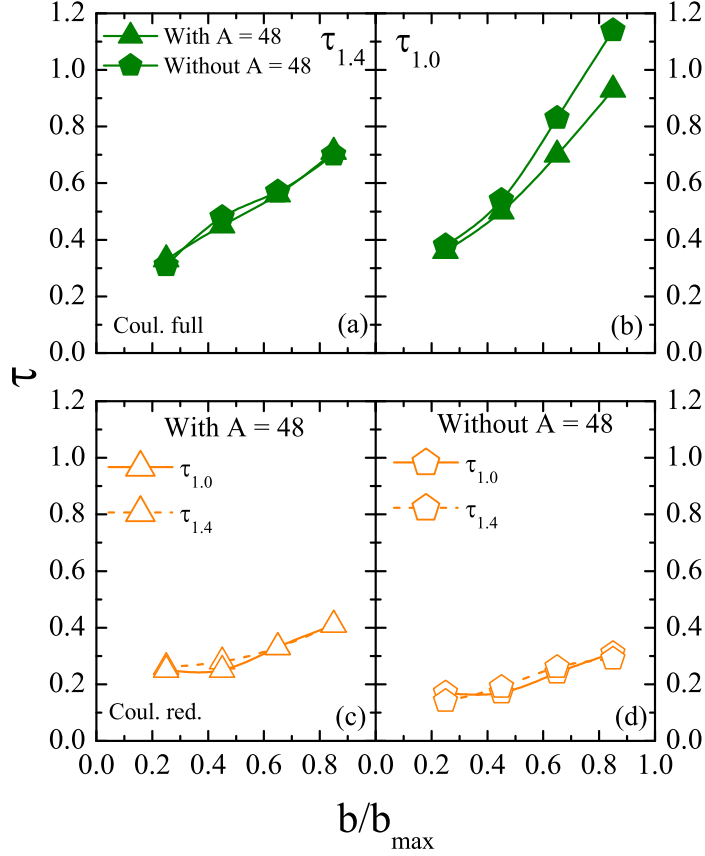


Figure 2: (Color online) Upper (lower) panels display τ as a function of reduced impact parameter for full (reduced) Coulomb. Values are plotted at upper limit of each bin. Symbols are explained in text. Lines are only to guide the eye.

energy in isospin effects on E_{bal} as well as its mass dependence at semi central colliding geometry (BIN 2). Since here we plan to extend that study over a full range of colliding geometry, so here also we reduce the Coulomb potential by a factor of 100 and calculate the E_{bal} throughout the mass range at all colliding geometries. Solid (open) diamonds represent E_{bal} calculated with reduced Coulomb for systems with lower (higher) neutron content. Lines are power law fit $\propto A^\tau$. Interestingly, we find that:

(a) the magnitude of isospin effects (difference in E_{bal} for a given pair) is now nearly same throughout the mass range which indicates that the effect of symmetry energy is uniform throughout the mass range. This is true for all the colliding geometries. This is supported

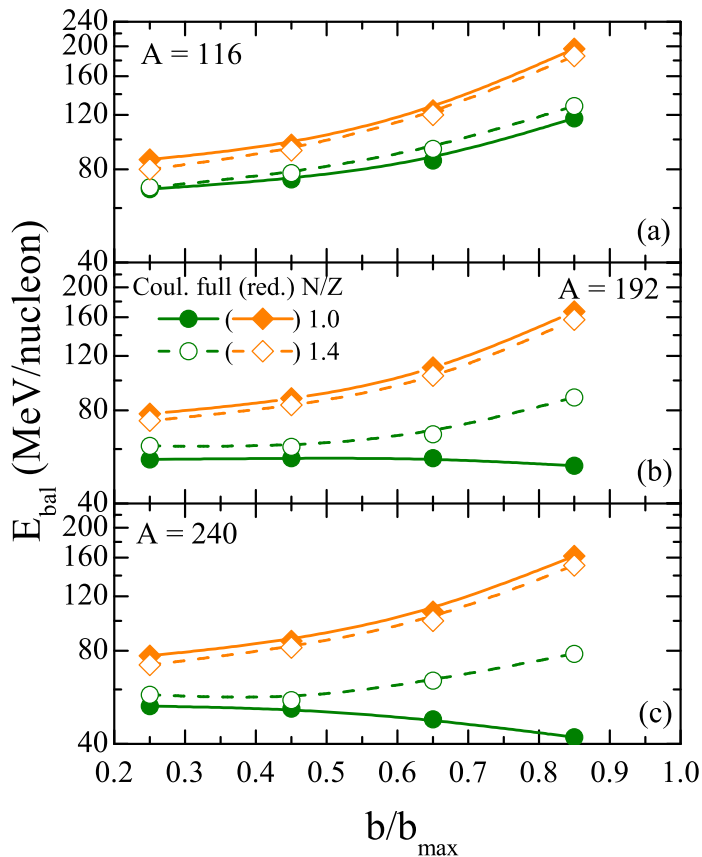


Figure 3: (Color online) E_{bal} as a function of impact parameter for different system masses. Various symbols have same meaning as in Fig.1. Lines are only to guide the eye.

by Ref. [17] where Sood and Puri studied the average density as a function of mass of the system (throughout the periodic table) at incident energies equal to E_{bal} for each given mass. There they found that although both E_{bal} and average density follows a power law behavior $\propto A^\tau$, E_{bal} decreases more sharply with the combined mass of the system (with $\tau = -0.42$), whereas the average density (calculated at incident energy equal to E_{bal}) is almost independent of the mass of the system with $\tau = -0.05$. It is worth mentioning here that the trend will be different at fixed incident energy in which case density increases with increase in the mass of the system [18, 19]. We also note that the power law with reduced Coulomb is now absolute for $N/Z = 1$ (solid diamonds fig. 1 (d)). This indicates that the deviations from power law behavior for heavy mass systems (with $N/Z = 1$) are

due to the dominance of Coulomb repulsion.

(b) one can also see that the enhancement in E_{bal} (by reducing Coulomb) is more in heavier systems as compared to lighter systems for all colliding geometries. The effect is more pronounced at higher colliding geometries.

(c) throughout the mass range at all colliding geometries, the neutron-rich systems have a decreased E_{bal} as compared to neutron-deficient systems when we reduce the Coulomb. This trend is quite the opposite to the one which we have when we have full Coulomb. This (as explained in Ref. [13] also) is due to the fact that the reduced Coulomb repulsion leads to higher E_{bal} . As a result, the density achieved during the course of the reaction will be more due to which the impact of the repulsive symmetry energy will be more in neutron-rich systems, which in turn leads to a decreased E_{bal} for neutron-rich systems.

Now to discuss how the value of τ changes if we exclude lighter systems (right panels in fig. 1), we display in fig. 2 the variation of τ as a function of impact parameter. Solid (open) symbols are for full (reduced) Coulomb. Triangles (pentagons) represent τ with (without) $A = 48$. For full Coulomb (upper left panel), $\tau_{1.4}$ increases with increase in impact parameter but the increase is independent of inclusion/exclusion of lighter mass. On the other hand, τ_1 increases drastically with impact parameter (upper right panel). Moreover, the increase in τ_1 (with impact parameter) is more sharp when we take into account only heavier masses (pentagons) as compared to when lighter mass systems are also included (triangles). Thus as we have discussed in Ref. [13] also that if we take into account only heavier systems, the value of τ is more as compared to if we include lighter systems as well. Here we see enhancement of this effect with increase in colliding geometry showing the increased role of Coulomb repulsion in mass dependence of E_{bal} at high impact parameter. In lower left panel, for reduced Coulomb, we see the values of τ_1 and $\tau_{1.4}$ increases much less sharply with increase in colliding geometry and this increase is almost independent of N/Z of the system which shows that the effect of isospin-dependent cross section and symmetry energy on the mass dependence of E_{bal} is independent of N/Z throughout the colliding geometry. The same is true if we consider only heavier systems as well (lower right panel). As we have seen in fig. 1, the effect of symmetry energy is uniform throughout the mass range at all colliding geometries, this means that the effect of cross section must also be nearly same through the mass range and colliding geometry. We will come to this point later. It is worth mentioning that since IQMD reproduces the data nicely [11] so the experimental values of tau are not expected to differ much from

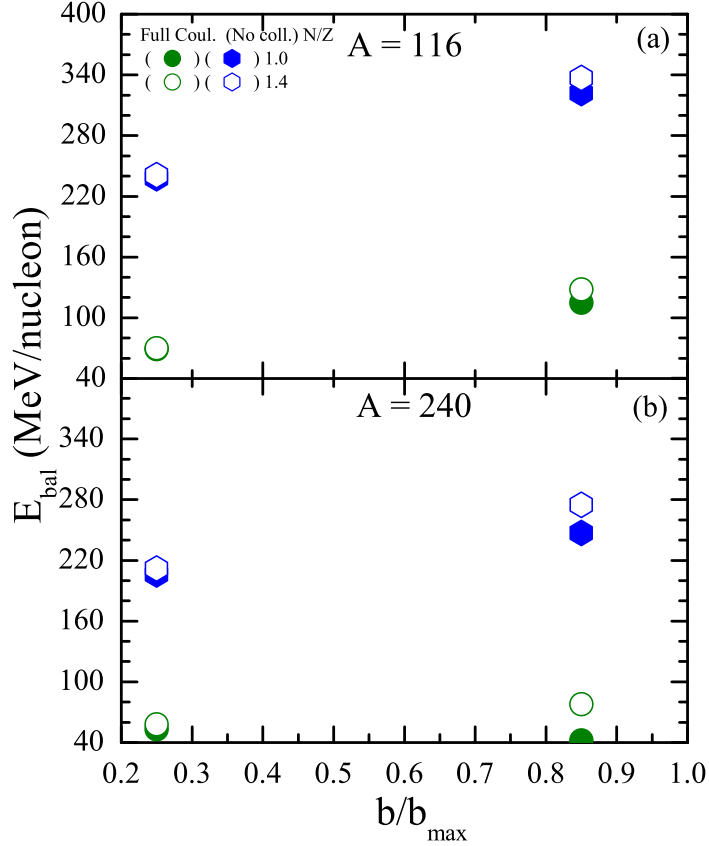


Figure 4: (Color online) E_{bal} at central and peripheral colliding geometries for $A = 116$ (upper panel) and $A = 240$ (lower panel) with no nucleon-nucleon collisions (Hexagons). Circles represent the calculations with collisions.

the values of tau given in table 1.

In fig. 3a, 3b, and 3c, we display E_{bal} as a function of \hat{b} for masses 116, 192, and 240, respectively, for both full and reduced Coulomb. Symbols have the same meaning as in fig. 1. For full Coulomb (green circles), for all the masses at all colliding geometries, system with higher N/Z has larger E_{bal} in agreement with previous studies [8, 9, 20]. Moreover, the difference between E_{bal} for a given mass pair, increases with increase in colliding geometry. This is more clearly visible in heavier masses. Also for N/Z = 1.4, E_{bal} increases with increase in impact parameter in agreement with Ref. [20]. This is due to the decreased participant zone in peripheral collisions which decreases the amount of repulsive

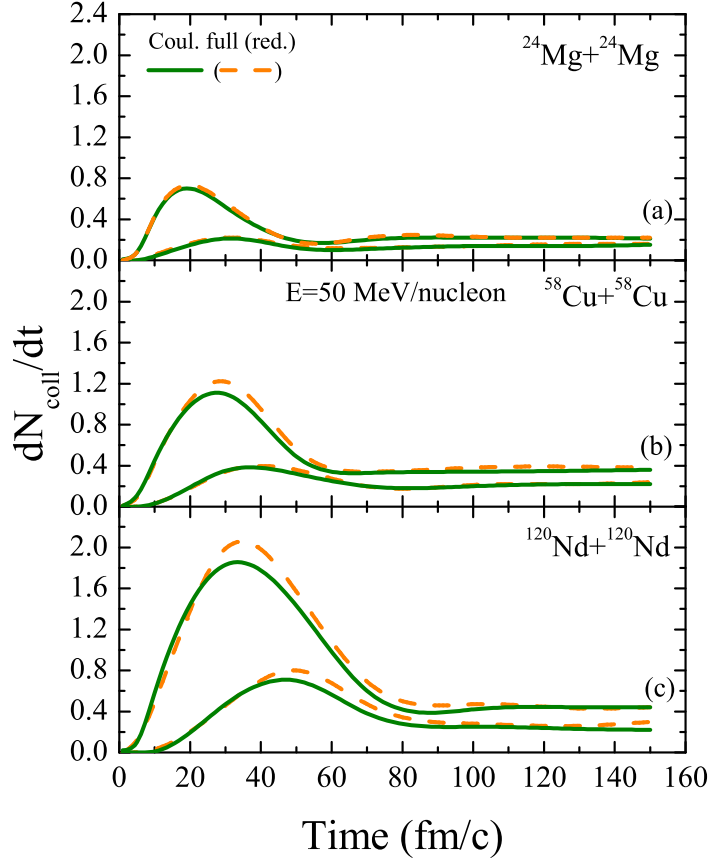


Figure 5: (Color online) The time evolution of collision rate ($\frac{dN_{coll}}{dt}$) for various system masses at 50 MeV/nucleon for BIN 1 and BIN 4. Various lines are explained in the text .

nn collisions and therefore higher energy is required to overcome the attractive nuclear force. This effect is less pronounced in heavier systems since even at peripheral geometry significant number of nn collisions will occur. Moreover, the effect of stronger Coulomb repulsion in heavier systems will increase with colliding geometry since it will push more number of nucleons in the transverse direction away from participant zone. However for $N/Z = 1$, increase in E_{bal} with impact parameter is true only for lighter mass system such as $A = 116$. For heavier masses E_{bal} infact begins to decrease with increase in impact parameter in contrast to the previous studies [8, 9, 11, 20]. However, when we reduce the Coulomb (by a factor of 100 (diamonds)), we find that:

(i) Neutron-rich systems have a decreased E_{bal} as compared to neutron-deficient systems as mentioned previously also. This is true at all the colliding geometries throughout the mass range. This clearly shows the dominance of Coulomb repulsion over symmetry energy in isospin effects throughout the mass range at all colliding geometries.

(ii) The difference between E_{bal} for systems with different N/Z remains almost constant as a function of colliding geometry which indicates that the effect of symmetry energy is uniform throughout the range of \hat{b} as well. This also shows that the large differences in E_{bal} values for a given isobaric pair are due to the Coulomb repulsions.

(iii) In heavier systems, at high colliding geometry, the increase in E_{bal} is more in systems with $N/Z = 1$ compared to $N/Z = 1.4$ which shows the much dominant role of Coulomb repulsion at high colliding geometry.

To see the relative contribution of Coulomb repulsion and cross section in lighter and heavier systems, we switch off the collision term and calculate the E_{bal} for $A = 116$ and 240 at two extreme bins. The results are displayed in fig. 4. Hexagons represent the calculations without collisions. Other symbols have same meaning as in fig. 1. We find that at a given impact parameter E_{bal} increases by large magnitude for both systems which shows the importance of collisions. The increase is of the same order for both the masses at both impact parameter bins indicating the same role of cross section for both lighter and heavier masses as we have expected in discussion of fig. 2. This is supported by Ref. [17, 18], which shows that since mean field is independent of the mass of the system, so one needs the same amount of collisions to counter balance the mean field in both lighter and heavier masses. Moreover, the same order of increase of E_{bal} at central and peripheral colliding geometry (when we switch off the collisions) indicates the importance of collisions at high colliding geometry as well. The effect that E_{bal} decreases with increase in impact parameter (due to dominance of Coulomb) for heavy mass systems with $N/Z = 1$ (fig. 3 lower panel) does not appear here for lighter and heavier masses. Therefore in fig. 3, the reduced Coulomb allows one to examine the balance of nn collisions and mean field while in fig. 4 the removal of nn collisions allows one to examine the balance of Coulomb and mean field.

As we have seen in fig. 4 that E_{bal} is much higher than the actual E_{bal} when we switch off the cross section, so to explore whether Coulomb repulsion affects the collisions in the E_{bal} domain, we display in fig. 5 collision rate $\frac{dN_{coll}}{dt}$ for $A = 48$ (upper panel), 116 (middle panel), and 240 (bottom panel) at incident energy of 50 MeV/nucleon. Solid (dashed)

lines represent Coulomb full (reduced) calculations. Higher (lower) peaks represent results for central (peripheral) impact parameter. We find that Coulomb decreases the collision rate in medium and heavier mass systems for central bins whereas for peripheral bins, the effect of Coulomb on collisions is only for heavier masses (lower panel). Comparing top and bottom panel we see that there are still significant number of collisions at peripheral geometry.

4 Summary

We have studied the isospin effects in the disappearance of flow as well as its mass dependence throughout the mass range 48-270 for two sets of isobaric systems with $N/Z = 1$ and 1.4 in the whole range of colliding geometry. Our results clearly demonstrate the dominance of Coulomb repulsion in isospin effects on E_{bal} as well as its mass dependence throughout the range of colliding geometry. The above study also shows that the effect of symmetry energy on E_{bal} and cross section is uniform throughout the mass range and colliding geometry. We have also presented the counter balancing of nn collisions and mean field by reducing the Coulomb and the counter balancing of Coulomb and mean field by removing the nn collisions.

This work has been supported by a grant from Indo-French Centre For The Promotion Of Advanced Research (IFCPAR) under project no. 4104-1.

References

- [1] W. Zhan *et al.*, Int. J. Mod. Phys. E **15**, 1941 (2006); see, e.g. <http://www.impcas.ac.cn/zhuye/en/htm/247.htm>.
- [2] See, e.g., <http://www.gsi.de/fair/indexe.html>.
- [3] Y. Yano, Nucl. Inst. Methods B **261**, 1009 (2007).
- [4] See, e.g., <http://www.ganil-spiral2.eu/research/developments/spiral2/>.
- [5] See, e.g., White Papers of the 2007 NSAC Long Range Plan town Meeting, Jan. 2007, Chiacgo, <http://dnp.aps.org>.
- [6] B. A. Li, L. W. Chen, and C. M. Ko, Phys. Rep. **464**, 113 (2008) and refernces within.

- [7] D. Krofcheck *et al.*, Phys. Rev. Lett. **63**, 2028 (1989).
- [8] B. A. Li, Z. Ren, C. M. Ko, and S. J. Yennello., Phys. Rev. Lett. **76**, 4492 (1996).
- [9] R. Pak *et al.*, Phys. Rev. Lett. **78**, 1022 (1997); *ibid.* **78**, 1026 (1997).
- [10] F. Daffin and W. Bauer, arxiv: 9809.0241v1.
- [11] S. Gautam, R. Chugh, A. D. Sood, R. K. Puri, C. Hartnack, and J. Aichelin, J. Phys. G: Nucl. Part. Phys. **37**, 085102 (2010).
- [12] C. Hartnack, R. K. Puri, J. Aichelin, J. Konopka, S. A. Bass, H. Stöcker, and W. Greiner, Eur. Phys. J. A **1**, 151 (1998).
- [13] S. Gautam and A. D. Sood, Phys. Rev. C **82**, 014604 (2010).
- [14] A. D. Sood, to be submitted.
- [15] A. D. Sood and R. K. Puri, Phys. Lett. **B594**, 260 (2004); *ibid.*, Eur. Phys. J. A **30**, 571 (2006).
- [16] E. Lehmann, A. Faessler, J. Zipprich, R. K. Puri, and S. W. Huang, Z. Phys. A **355**, 55 (1996).
- [17] A. D. Sood and R. K. Puri, Phys. Rev. C **70**, 034611 (2004).
- [18] B. Blättel *at al.*, Phys. Rev. C **43**, 2728 (1991).
- [19] D. T. Khoa *et al.*, Nucl. Phys. **A542**, 671 (1992).
- [20] D. J. Magestro, W. Bauer, and G. D. Westfall, Phys. Rev. C **62**, 041603(R) (2000); R. Chugh and R. K. Puri, Phys. Rev. C **82**, 014603 (2010); D. Klakow, G. Welke, and W. Bauer, Phys. Rev. C **48**, 1982 (1993).